Biogeosciences Discuss., doi:10.5194/bg-2015-558, 2016
Manuscript under review for journal Biogeosciences
Published: 18 January 2016

Biogeosciences Discussions
Open Access
EGU

Controls of longitudinal variation in δ^{13}C-DIC in rivers: A global meta-analysis

K. A. Roach[1], M. A. Rodríguez[1], Y. Paradis[2], and G. Cabana[1]

[1] {Université du Québec à Trois-Rivières, Département des sciences de l'environnement, C.P. 500, Trois-Rivières, Québec G9A 5H7, Canada}

[2] {Ministère des Forêts, de la Faune et des Parcs, 880, Chemin Ste-Foy, Québec City, Québec G1S 4X4, Canada}

Correspondence to: K. A. Roach (roackat@gmail.com)

Abstract

We conducted a literature survey to investigate controls and spatial and temporal patterns of δ^{13}C-DIC and deviations between δ^{13}C-DIC and the δ^{13}C signature of DIC at isotopic equilibrium with the atmosphere ($\Delta\delta^{13}$C-DIC) in streams and rivers throughout the world. We used generalized additive mixed models to relate $\Delta\delta^{13}$C-DIC and δ^{13}C-DIC in lotic ecosystems to ecological variables including elevation, Strahler order, and partial pressure of dissolved CO_2 (pCO_2), and to examine seasonal shifts in $\Delta\delta^{13}$C-DIC and δ^{13}C-DIC over a range in latitude. Elevation, Strahler order, and DIC concentrations explained a large fraction of the variation in $\Delta\delta^{13}$C-DIC, and these variables plus pH and pCO_2 explained much of the variation in δ^{13}C-DIC. Seasonal fluctuations in δ^{13}C-DIC were most apparent in rivers located in temperate regions with seasonal snow cover. Small streams tended to have lower δ^{13}C-DIC values than large rivers. Overall, our analysis indicates that processes that add CO_2 to the water column, including groundwater inputs, decomposition, and respiration, should have a greater influence on δ^{13}C-DIC

Biogeosciences Discuss., doi:10.5194/bg-2015-558, 2016
Manuscript under review for journal Biogeosciences
Published: 18 January 2016

than processes that remove CO_2. Both physical (gas exchange with the atmosphere, weathering, ice cover) and biological (respiration in regions with high C_4 grass abundance, photosynthesis by cyanobacteria) processes appear to control δ^{13}C-DIC in streams and rivers, but the relative importance of these processes shifts from upstream to downstream.

Key words: biogeochemistry, carbon, generalized additive mixed model, river, stable isotope

1 Introduction

Stable isotope analysis of carbon (δ^{13}C) is widely used to investigate biogeochemical cycling and food web dynamics in aquatic ecosystems. Geological, atmospheric, and biological sources of dissolved inorganic carbon (DIC) often have unique isotopic signatures (Boutton 1991); consequently, δ^{13}C is a valuable tracer of the origin of DIC. The δ^{13}C signature of DIC (δ^{13}C-DIC) in the water column can be altered by the addition of DIC with a distinctive δ^{13}C signature and by processes that affect the relative abundance of ^{13}C:^{12}C (fractionation). The resulting spatial variation in δ^{13}C-DIC yields important information about the carbon cycle. In addition to being of interest to biogeochemists, large-scale spatial gradients of δ^{13}C have been used by ecologists in trophic applications. Agreement in δ^{13}C between consumer tissues and DIC along a fluvial isotope gradient has been used to estimate the spatial scale of consumer feeding movements (Rasmussen et al., 2009; Bertrand et al., 2011). The δ^{13}C signature of algae often tracks the longitudinal gradient in δ^{13}C-DIC, whereas δ^{13}C of terrestrial-based detritus is relatively constant over space (Gray et al., 2011). Recent stable isotope mixing models use the upstream-downstream gradient in δ^{13}C-DIC to estimate contributions of algal versus terrestrial production sources to consumer biomass by assuming that consumer δ^{13}C is a weighted mixture

Biogeosciences Discuss., doi:10.5194/bg-2015-558, 2016
Manuscript under review for journal Biogeosciences
Published: 18 January 2016

of algal and terrestrial signature gradients (Rasmussen, 2010). A better understanding of controls and spatial and temporal patterns of δ^{13}C-DIC in rivers would facilitate the use of δ^{13}C as a natural tracer.

Gas exchange with the atmosphere is one mechanism that might strongly influence δ^{13}C-DIC in rivers. Exchange of CO_2 between the water and the atmosphere causes fractionation between different carbonate species that is dependent on pH and temperature (Zhang et al., 1995). At isotopic equilibrium with the atmosphere, $CO_{2\ (aq)}$ has a lower δ^{13}C signature relative to HCO_3^- and CO_3^{2-}. In streams with neutral to basic pH (dominant in HCO_3^-), this process yields $DIC_{(aq)}$ with a relatively high δ^{13}C signature. Other physical processes influencing δ^{13}C-DIC in rivers include carbonate mineral weathering and mixing of different water bodies. Carbonate weathering, the formation of HCO_3^- via the dissolution of carbonate minerals, produces DIC with a relatively high δ^{13}C signature, reflecting δ^{13}C of carbonate rocks (Kendall and Doctor, 2003). Influx of a water body also can influence δ^{13}C-DIC in the recipient system. For example, groundwater is supersaturated in $CO_{2\ (aq)}$ from soil respiration and decomposition of organic matter (Wanninkhof et al., 1990), and its input lowers δ^{13}C-DIC.

Biological processes, including heterotrophic respiration, decomposition of organic matter, and algal primary production also cause changes in δ^{13}C-DIC. Whereas DIC derived from heterotrophic respiration and decomposition has a low δ^{13}C signature, algae preferentially use ^{12}C over ^{13}C during photosynthesis, yielding DIC with a high δ^{13}C signature (McKenzie, 1985). Other studies have indicated that in productive rivers, high demand for CO_2 by algae promotes invasion of atmospheric CO_2 into the water column (Finlay, 2003; Roussel et al., 2013). Thus, productive rivers tend to have low pCO_2 values due to algae uptake and δ^{13}C-DIC values that are near isotopic equilibrium with the atmosphere ($\delta^{13}C\text{-}DIC_{equilibrium}$) (Finlay, 2003).

Biogeosciences Discuss., doi:10.5194/bg-2015-558, 2016
Manuscript under review for journal Biogeosciences
Published: 18 January 2016

Deviations between δ^{13}C-DIC and the δ^{13}C signature of DIC at isotopic equilibrium with the atmosphere ($\Delta\delta^{13}$C-DIC) should reveal biological control of δ^{13}C-DIC in streams and rivers. Sites from rivers with high algal primary production and low pCO_2 would be expected to be closest to $\delta^{13}C\text{-}DIC_{equilibrium}$.

A number of studies in lotic ecosystems have shown that δ^{13}C-DIC undergoes a predictable shift from upstream to downstream, with headwaters having lower δ^{13}C-DIC values than further downstream (Yang et al., 1996; Telmer and Veizer, 1999; Finlay, 2003). In a study of the Ottawa River Basin in Canada, Telmer and Veizer (1999) found that δ^{13}C-DIC in upland tributaries dominated by silicate lithology was -16‰, and δ^{13}C-DIC in the lowland main channel dominated by carbonate lithology was -8‰. Similarly, in a survey of streams and rivers in Northern California, USA, Finlay (2003) found that δ^{13}C-DIC and $CO_{2\,(aq)}$ increased with discharge. DIC dynamics in rivers may respond to shifts along the upstream-downstream gradient in environmental factors. For example, Telmer and Veizer (1999) concluded that soil respiration and carbonate weathering produced much of the longitudinal variation in δ^{13}C-DIC, and that CO_2 exchange between the water and atmosphere and instream primary production were relatively unimportant. Finlay (2003) suggested that groundwater inputs, outgassing (evasion) of excess CO_2, and microbial respiration primarily control δ^{13}C-DIC in small streams, whereas algal photosynthesis and CO_2 exchange with the atmosphere become more important in large rivers. An increase in carbonate weathering, a decline in groundwater inputs, CO_2 loss to the atmosphere, and increasing rates of algal primary production are all associated with a decline in $CO_{2\,(aq)}$ concentrations with increasing river size (Jones and Mulholland, 1998; Dawson et al., 2001), making the relative influence of these processes on δ^{13}C-DIC difficult to parse out.

In addition to having high spatial heterogeneity, rivers are temporally dynamic.

Biogeosciences Discuss., doi:10.5194/bg-2015-558, 2016
Manuscript under review for journal Biogeosciences
Published: 18 January 2016

93 Floodplain rivers in particular show strong seasonality resulting from changes in river-floodplain
94 connectivity. Flood stage has a strong impact on several major processes influencing δ^{13}C-DIC,
95 including ecosystem metabolism, the fraction of groundwater relative to total discharge volume,
96 and decomposition of organic matter. Several studies have identified seasonal shifts in δ^{13}C-DIC
97 that are comparable to longitudinal variation in δ^{13}C-DIC. In lowland reaches of the Okavango
98 River in Botswana, decomposition of terrestrial organic matter contributes to δ^{13}C-DIC values
99 that are 4‰ lower during the annual period of floodplain inundation (Akoko et al., 2013). In the
100 St. Lawrence River in Canada, seasonality in algal primary production and respiration in soils
101 and groundwater causes δ^{13}C-DIC values to shift from -6.8‰ in spring to -1.0‰ in autumn
102 (Hélie et al., 2002).

103 We conducted a literature survey of $\Delta\delta^{13}$C-DIC and δ^{13}C-DIC in lotic ecosystems
104 throughout the world, with the aim of contrasting the physical and biological processes
105 controlling $\Delta\delta^{13}$C-DIC and δ^{13}C-DIC in streams and in large rivers. We used generalized
106 additive mixed models (GAMMs; Wood, 2006) to relate $\Delta\delta^{13}$C-DIC and δ^{13}C-DIC in lotic
107 ecosystems to ecological variables including elevation, Strahler order, and the partial pressure of
108 dissolved CO_2 (pCO_2), and to examine seasonal shifts in $\Delta\delta^{13}$C-DIC and δ^{13}C-DIC over a range
109 in latitude. We originally expected that if δ^{13}C-DIC was mainly under biotic control, we would
110 find a negative relationship between pCO_2 and $\Delta\delta^{13}$C-DIC.

111

112 ## 2 Methods

113 ### 2.1 Literature survey

114 We collated data from the scientific literature using the search engines Google Scholar and
115 Web of Science and using the search terms “river”, “stable isotope”, and “dissolved inorganic

Biogeosciences Discuss., doi:10.5194/bg-2015-558, 2016
Manuscript under review for journal Biogeosciences
Published: 18 January 2016

carbon". We recorded data directly from tables or interpolated data from figures and maps using data extraction software (GraphClick v.3.0.2) and Google Earth. For each site we recorded geographic coordinates, δ^{13}C-DIC, temperature, pH, alkalinity, pCO_2, DIC concentrations, and day-of-the-year of sample collection. If pCO_2 was not provided, we calculated it from pH, alkalinity, and temperature (Stumm and Morgan, 2012). For the studies that only provided the month or season of sampling, we used the midpoint of month or season as an estimate of day-of-the-year. We were mainly interested in investigating controls of DIC cycling in the main channel of rivers and thus eliminated sites from natural lakes. Our search yielded a total of 1,530 δ^{13}C-DIC values from 26 publications (Appendix 1). Our dataset has a nested structure, with sites (n = 801) nested within rivers (n = 302), which are nested within watersheds (n = 31). Watersheds were located in Africa (4), Asia (4), Australia (1), Europe (6), North America (7), and South America (9) (Fig. 1).

The δ^{13}C-DIC signature at isotopic equilibrium with the atmosphere, $\delta^{13}C\text{-}DIC_{equilibrium}$, was calculated from Zhang et al. (1995) using the equations $\varepsilon CO_{2(aq)} - CO_{2(gas)} = -0.0049 \times T - 1.31$, $\varepsilon HCO_3^- - CO_{2(gas)} = -0.141 \times T + 10.78$, and $\varepsilon CO_3^- - CO_{2(gas)} = -0.052 \times T + 7.22$, where T is temperature in °C. We assumed a δ^{13}C signature of -7.8 for atmospheric CO_2 (Levin et al. 1987). The proportion of each DIC species was then weighted using the equation $\delta^{13}C_{DIC} = \sum f_i \varepsilon_i$, where f is the proportion of each species (i) and ε is the permil fractionation. We used the proportion of DIC species estimated from pH and temperature (Stumm and Morgan, 2012) to determine $\delta^{13}C\text{-}DIC_{equilibrium}$.

We used a geographic information system to determine elevation (masl), Strahler order, and channel distance from river mouth for each site. We characterized Strahler order using the 15-sec river network data from HydroSHEDS, a hydrographic database derived from elevation

Biogeosciences Discuss., doi:10.5194/bg-2015-558, 2016
Manuscript under review for journal Biogeosciences
Published: 18 January 2016

data (Lehner et al., 2008). The majority of sites were at low elevation (i.e., 82% were at < 500 masl), but the highest-elevation sites (> 3500 masl) were from second or third order streams. Rivers with Strahler order > 4 accounted for 44% of the sites in our literature survey. In the northern hemisphere, < 1% of sites were collected from rivers in polar regions (latitude > 66.5°), 72% were from temperate regions (latitude 23.5° to 66.5°), and 7% were from tropical regions (latitude 0° to 23.5°) (Fig. 1). In the southern hemisphere, no sites were collected from polar regions, 5% were from temperate regions, and 16% were from tropical regions.

2.2 Generalized additive mixed models

Sites were spatially nested within rivers and watersheds, requiring us to account for intra-group correlations in our statistical analyses. By adding random effects to the additive predictor, GAMMs enable modeling of overdispersed and correlated data that frequently arise in spatial analyses (Wood, 2006). Before constructing GAMMs, we examined correlations among the explanatory variables using matrix scatterplots and transformed strongly skewed variables to reduce the influence of extreme values.

We constructed separate GAMMs relating $\Delta\delta^{13}$C-DIC and δ^{13}C-DIC to all the explanatory variables. We then iteratively removed variables if 95% confidence intervals for the smooth function included zero throughout the range of measured values, and re-fitted the model until the zero line was not entirely contained by the confidence interval for all variables. The GAMMs for $\Delta\delta^{13}$C-DIC and δ^{13}C-DIC both had δ^{13}C-DIC as the dependent variable, but models for $\Delta\delta^{13}$C-DIC additionally included $\delta^{13}C\text{-}DIC_{equilibrium}$ as an offset. We allowed for different seasonal patterns in $\Delta\delta^{13}$C-DIC and δ^{13}C-DIC in the Northern and Southern hemispheres by including the interaction between day of the year and latitude in the GAMMs. We modeled seasonality and

Biogeosciences Discuss., doi:10.5194/bg-2015-558, 2016
Manuscript under review for journal Biogeosciences
Published: 18 January 2016

latitudinal effects as cosinor functions of day-of-year and latitude (Barnett and Dobson, 2010) comprising sine and cosine terms because measurements on a linear scale do not adequately represent the circular nature of these variables (e.g., the equal spacing between days-of-year 365, 1, and 2 is not captured by the linear scale).

All GAMMs were fit with an identity link function, a normal distribution for errors, and a penalized regression spline (Wood, 2006, 2011). We incorporated Strahler order as a simple linear effect and river and watershed as random effects. Distance from river mouth (river km) was included as a covariate to account for smaller-scale spatial correlation. We used restricted maximum likelihood estimation (REML) to fit GAMMs. Potential explanatory variables for $\Delta\delta^{13}$C-DIC included elevation, Strahler order, pCO_2, DIC, and the interaction between latitude and day of the year. Potential explanatory variables for δ^{13}C-DIC included elevation, Strahler order, temperature, pH, pCO_2, DIC, and the interaction between latitude and day of the year. The final models were:

$$\delta^{13}\text{C-DIC} = \log_e(\text{DIC}) + \beta_0 + \beta_1\ \text{Strahler order} + f(\log_e(\text{Elevation} + 8)) + f(\sin(\pi \times \text{Day-of-year}/365), \sin(\pi \times \text{Latitude}/180)) + f(\cos(\pi \times \text{Day-of-year}/365), \cos(\pi \times \text{Latitude}/180)) + f(\log_e(\text{Distance from river mouth} + 1)) + f(\text{Watershed}) + f(\text{River}) + \varepsilon$$

for $\Delta\delta^{13}$C-DIC, and

$$\delta^{13}\text{C-DIC} = \beta_0 + \beta_1\ \text{Strahler order} + f(\text{pH}) + f(\log_e(pCO_2)) + f(\log_e(\text{Elevation} + 8)) + f(\sin(\pi \times \text{Day-of-year}/365), \sin(\pi \times \text{Latitude}/180)) + f(\cos(\pi \times \text{Day-of-year}/365), \cos(\pi \times \text{Latitude}/180)) + f(\log_e(\text{Distance from river mouth} + 1)) + f(\text{Watershed}) + f(\text{River}) + \varepsilon$$

Biogeosciences Discuss., doi:10.5194/bg-2015-558, 2016
Manuscript under review for journal Biogeosciences
Published: 18 January 2016

185

186 for δ^{13}C-DIC.

187

188 In the models, $\log_e$(DIC) is an offset, β are regression coefficients, *f*(.) are smooth
189 functions, *f*(Watershed) and *f*(River) represent random effects, and ε is normally distributed
190 error. We used R software (R Development Core Team, 2015) for all statistical analyses and the
191 mgcv package to generate GAMMs (Wood 2011).

192

193 **3 Results**

194 In the literature survey, δ^{13}C-DIC ranged from -28.1‰ to 0.7‰. δ^{13}C-$DIC_{equilibrium}$ ranged
195 from -10.6‰ to 2.9‰, and thus did not capture the full variation in δ^{13}C-DIC (Fig. 2). Many of
196 the sites from lowland rivers, including the Indus, Negro (Argentina), Okavango, Santa Cruz,
197 and St. Lawrence rivers, had δ^{13}C-DIC values that were near δ^{13}C-$DIC_{equilibrium}$ (Fig. 2).
198 However, other sites from lowland rivers, including the Slave and Madeira rivers, had δ^{13}C-DIC
199 that was considerably lower than δ^{13}C-$DIC_{equilibrium}$.

200 The GAMM of $\Delta\delta^{13}$C-DIC modeled deviations between δ^{13}C-DIC and δ^{13}C-
201 $DIC_{equilibrium}$. Explanatory variables retained in this GAMM included elevation, Strahler order,
202 DIC, and the interaction between latitude and day of the year (Table 1). The final GAMM for
203 $\Delta\delta^{13}$C-DIC included 889 data points from the literature survey; the model explained a total of
204 85% of the deviance and showed good agreement between fitted and observed values (Fig. 3).

205 The GAMM of $\Delta\delta^{13}$C-DIC indicated that sites at the lowest and highest elevations were
206 closer to δ^{13}C-$DIC_{equilibrium}$ (Fig. 4). $\Delta\delta^{13}$C-DIC values were positively related to river size, as
207 measured by Strahler order, indicating that streams tended to have δ^{13}C-DIC that was far from

Biogeosciences Discuss., doi:10.5194/bg-2015-558, 2016
Manuscript under review for journal Biogeosciences
Published: 18 January 2016

208 δ^{13}C-DIC$_{equilibrium}$ and large rivers tended to have δ^{13}C-DIC that was near δ^{13}C-DIC$_{equilibrium}$ (Fig.
209 5). Sites with high DIC concentrations also tended to be near δ^{13}C-DIC$_{equilibrium}$, as shown by
210 high $\Delta\delta^{13}$C-DIC values (Fig. 4). The relationship between DIC concentration and $\Delta\delta^{13}$C-DIC
211 was not linear. There was a positive relationship between DIC and $\Delta\delta^{13}$C-DIC at low
212 concentrations (0.05 to 0.20 mmol/L), and no relationship between DIC and $\Delta\delta^{13}$C-DIC for
213 concentrations > 0.20 mmol/L. Seasonal variation in $\Delta\delta^{13}$C-DIC was apparent in rivers located in
214 temperate regions from 40° to 60°N and -60° to -40°S (Fig. 6). In the northern hemisphere from
215 40° to 60°, $\Delta\delta^{13}$C-DIC values were lowest during the winter and early spring (i.e., from January
216 to April). In the southern hemisphere from 40 to 60°, $\Delta\delta^{13}$C-DIC values were lowest from
217 January to August and highest during the spring and early summer (i.e., from September to
218 December). Tropical rivers tended to have lower $\Delta\delta^{13}$C-DIC values than temperate rivers. The
219 highest $\Delta\delta^{13}$C-DIC fitted values were for rivers located from 40° to 60°N during September to
220 December.

221 Explanatory variables retained in the model for δ^{13}C-DIC included elevation, Strahler
222 order, pCO_2, DIC, pH, and the interaction between latitude and day of the year (Table 2). The
223 final GAMM for δ^{13}C-DIC included 890 data points from the literature survey; the model
224 explained a total of 91% of the deviance and showed good agreement between fitted and
225 observed values (Fig. 3).

226 The GAMM of δ^{13}C-DIC showed that sites at the lowest and highest elevations tended to
227 have high δ^{13}C-DIC values (Fig. 7). δ^{13}C-DIC values were positively related to river size, as
228 measured by Strahler order (Fig. 5). δ^{13}C-DIC was related negatively to pCO_2 and positively to
229 DIC (Fig. 7). Again, the relationship between DIC concentrations and δ^{13}C-DIC was nonlinear.
230 There was a positive relationship between DIC and δ^{13}C-DIC at low concentrations (0.05 to 0.20

Biogeosciences Discuss., doi:10.5194/bg-2015-558, 2016
Manuscript under review for journal Biogeosciences
Published: 18 January 2016

mmol/L), and a weakly positive relationship between DIC and δ^{13}C-DIC at higher concentrations (0.20 to 7.5 mmol/L). The relationship between pH and δ^{13}C-DIC also was nonlinear. Sites with lowest and highest pH tended to have low δ^{13}C-DIC values (Fig. 7). Seasonal patterns in δ^{13}C-DIC and $\Delta\delta^{13}$C-DIC were very similar (Fig. 6).

4 Discussion

Our main objective was to investigate controls and spatial and temporal patterns of δ^{13}C-DIC in rivers throughout the world. pCO2 explained a large fraction of the deviance in the GAMM of δ^{13}C-DIC, but was not retained in the GAMM of $\Delta\delta^{13}$C-DIC, suggesting that algal primary production has limited control over δ^{13}C-DIC. However, as we will discuss below, our results provide evidence that other biological processes, including photosynthesis by cyanobacteria and respiration in regions with high C_4 grass abundance are important determinants of δ^{13}C-DIC in rivers (Fig. 8). Our results revealed changes in the dominant processes influencing δ^{13}C-DIC from upstream to downstream. Furthermore, we found that δ^{13}C-DIC changed seasonally in rivers in temperate regions with seasonal snow cover.

$\Delta\delta^{13}$C-DIC values were low (δ^{13}C-DIC was near $\delta^{13}C\text{-}DIC_{equilibrium}$) in high-elevation streams and large rivers, indicating that exchange of CO_2 between surface water and the atmosphere occurs via invasion or evasion in these systems. Most studies show that lotic ecosystems are supersaturated in pCO_2 (Richey et al., 2002; Jones et al., 2003; Cole et al., 2007) and are sources, not sinks, of CO_2 to the atmosphere (Mulholland et al., 2001; Battin et al., 2008). Thus, in most low-order streams, high $CO_{2\,(aq)}$ concentrations originating from inputs of groundwater and terrestrial soil water from sediments (e.g., Jones and Mulholland, 1998) result in high $\Delta\delta^{13}$C-DIC values, indicating that δ^{13}C-DIC is far from $\delta^{13}C\text{-}DIC_{equilibrium}$. In high-

Biogeosciences Discuss., doi:10.5194/bg-2015-558, 2016
Manuscript under review for journal Biogeosciences
Published: 18 January 2016

elevation streams, low $\Delta\delta^{13}$C-DIC values have been attributed to the high gradient and low surface:volume ratio, which increases water turbulence and promotes CO_2 outgassing (Rebsdorf et al., 1991; Dawson et al., 2004). For example, a recent estimate of gas transfer velocities in streams and rivers throughout the United States found that CO_2 outgassing is highest in headwater streams originating in areas with steep topography (Butman and Raymond, 2011). In small streams, groundwater consists of a large fraction of stream discharge, but its volume relative to the total volume of discharge decreases downstream (e.g., Devol et al., 1987; Johnson et al., 2006). $\Delta\delta^{13}$C-DIC values were likely low in large rivers because groundwater has less of an influence on water chemistry and because surface water has been exposed to the atmosphere for a relatively long period of time, promoting evasion of $CO_{2\,(aq)}$. $\Delta\delta^{13}$C-DIC values are particularly low in lacustrine rivers because the prolonged residence time of water in large lakes allows $CO_{2\,(aq)}$ to equilibrate with the atmosphere (Yang et al., 1996). $\Delta\delta^{13}$C-DIC values also were low in rivers with high DIC concentrations (> 0.2 mmol/L). In our dataset, DIC concentrations were strongly correlated with alkalinity (r = 0.98) and $CO_{2\,(aq)}$ concentrations did not have a strong effect on total DIC. $\Delta\delta^{13}$C-DIC values were probably low in rivers with high DIC concentrations because the carbon was derived from carbonate dissolution, which has a high δ^{13}C-DIC signature (Kendall and Doctor, 2003).

pCO_2 did not explain a large fraction of the total variation in $\Delta\delta^{13}$C-DIC, providing evidence that algal primary production does not control exchange of CO_2 between surface water and the atmosphere in most rivers. Calculation of pCO_2 from pH, alkalinity, and temperature results in values that are overestimated in acidic waters rich in dissolved organic carbon (Abril et al., 2015). In our meta-analysis, pCO_2 was calculated from these physicochemical variables in 90% of the studies. Direct measurements of pCO_2 in streams and rivers would allow for a more

Biogeosciences Discuss., doi:10.5194/bg-2015-558, 2016
Manuscript under review for journal Biogeosciences
Published: 18 January 2016

277 accurate assessment of the relationship between pCO_2 and $\Delta\delta^{13}$C-DIC. Although algal primary
278 production apparently did not cause invasion of atmospheric CO_2, low rates of photosynthesis
279 may have been sufficient to increase δ^{13}C-DIC values without increasing mixing of DIC between
280 the water and atmosphere. Some of the unexplained variation in the GAMM analysis of δ^{13}C-
281 DIC might have been caused by preferential assimilation of ^{12}C over ^{13}C by algae.

282 Our results showed that pCO_2 is negatively related to δ^{13}C-DIC. The spatial patterns in
283 δ^{13}C-DIC indicated by our analysis correspond to patterns in pCO_2 in streams and rivers that
284 have been observed elsewhere. For example, pCO_2 in rivers tends to decline downstream
285 (Raymond et al., 1997; Teodoru et al., 2009; Butman and Raymond, 2011), similar to the
286 relationship between δ^{13}C-DIC and Strahler order revealed by our analysis. Furthermore, tropical
287 rivers typically have higher concentrations of $CO_{2\ (aq)}$ than temperate rivers (Aufdenkampe et al.,
288 2011), similar to our results for latitudinal variation. The cycling of CO_2 has a strong influence
289 on the biogeochemistry of δ^{13}C-DIC; thus, processes that remove or add CO_2 to the water
290 column should also influence δ^{13}C-DIC. Major processes that remove CO_2 in lotic systems
291 include CO_2 evasion and algal primary production. In small streams, the major source of $CO_{2\ (aq)}$
292 is believed to be groundwater and terrestrial soil water, with *in situ* respiration and
293 decomposition of organic matter becoming more important in large rivers (Johnson et al., 2008;
294 Aufdenkampe et al., 2011). Most lotic systems are supersaturated in CO_2 and typically have low
295 δ^{13}C values relative to equilibrium with the atmosphere. Therefore, processes that add CO_2 to the
296 water column should generally have a greater influence on δ^{13}C-DIC than processes that remove
297 CO_2.

298 Similar to the spatial patterns in $\Delta\delta^{13}$C-DIC values, high-elevation streams and large
299 rivers had DIC with a high δ^{13}C signature. The congruent spatial trends between $\Delta\delta^{13}$C-DIC and

Biogeosciences Discuss., doi:10.5194/bg-2015-558, 2016
Manuscript under review for journal Biogeosciences
Published: 18 January 2016

300 δ^{13}C-DIC suggest that gas exchange influenced δ^{13}C-DIC in these systems. Our results also show
301 that DIC had a high δ^{13}C signature in rivers with high DIC concentrations. Large rivers likely
302 have high δ^{13}C-DIC values because their waters have higher concentrations of carbonate
303 minerals, and this higher buffering capacity inhibits decrease in δ^{13}C-DIC. Within a river
304 network, concentrations of dissolved ions are frequently heterogeneous among headwater
305 reaches, but tend to average out and increase downstream (Livingstone, 1963). Our results
306 indicated that sites with low and high pH had DIC with a low δ^{13}C signature. Many of the sites
307 with the lowest surface water pH (3.8 to 6.5) also tended to have low DIC concentrations (range
308 = < 0.1 to 2.5 mmol/L, average = 0.6 mmol/L). δ^{13}C-DIC values may have been low in rivers
309 with acidic surface water because these were blackwater rivers draining forested watersheds
310 dominated by igneous rock. In addition to having low pH, blackwater rivers have high
311 concentrations of dissolved organic matter that increase rates of microbial respiration (Meyer
312 1990), lowering δ^{13}C-DIC values. Sites with high pH and low δ^{13}C-DIC values also had low
313 pCO_2 (sites with pH > 9 had a maximum pCO_2 of 115 ppmv). When pH is high and pCO_2 is low,
314 intense photosynthesis by cyanobacteria can increase the rate of CO_2 invasion from the
315 atmosphere, producing fractionation that results in low δ^{13}C-DIC values (Herczog and Fairbanks,
316 1987). Following the depletion of free CO_2 that occurs in highly alkaline waters, cyanobacteria
317 can float on the water surface and use atmospheric CO_2 during carbon fixation (Paerl and Ustach,
318 1982). Lakes also exhibit a positive trend between pH and δ^{13}C-DIC until pH values of
319 approximately 8-9, at which point δ^{13}C-DIC decreases (Bade et al., 2004).

320 Rivers in the northern hemisphere between 40° and 60° exhibited seasonal cycles in
321 $\Delta\delta^{13}$C-DIC and δ^{13}C-DIC. In these rivers, $\Delta\delta^{13}$C-DIC and δ^{13}C-DIC values were lowest from
322 January to April, corresponding with the formation of ice cover. Studies of lakes have shown that

Biogeosciences Discuss., doi:10.5194/bg-2015-558, 2016
Manuscript under review for journal Biogeosciences
Published: 18 January 2016

duration of ice cover is an important control of seasonal patterns in pCO_2 and δ^{13}C-DIC. Ice insulates the lake from mixing by wind and gas exchange, which causes pCO_2 to increase in the water column and lowers δ^{13}C-DIC values (Striegl et al., 2001; Karlsson et al., 2008). The same phenomenon has been observed in terrestrial ecosystems, with snow cover increasing accumulation of CO_2 in the soil and lowering δ^{13}C-DIC values in the winter (Aravena et al., 1992). Ice cover also has been documented to increase pCO_2 in the water column of rivers (e.g., Raymond et al., 1997), and should be responsible for the seasonal shifts in $\Delta\delta^{13}$C-DIC and δ^{13}C-DIC values in rivers at high latitudes in the northern hemisphere. Sample size was low in temperate regions of the southern hemisphere. A greater number of sites sampled from these rivers may result in a seasonal trend that is similar to the pattern observed in the northern hemisphere. Our results also revealed that DIC has a lower δ^{13}C signature in many tropical rivers than in temperate rivers. An analysis of ^{13}C and ^{14}C of DIC, dissolved organic carbon, and multiple particulate organic carbon fractions in Amazonian rivers concluded that high pCO_2 was sustained by *in situ* respiration of terrestrial C_4 grasses (Mayorga et al., 2005). Terrestrial C_4 grasses decompose more rapidly than terrestrial C_3 plants (Wynn and Bird, 2007), and the high relative abundance of this group of macrophytes in the tropics promotes microbial respiration, lowering δ^{13}C-DIC values even during low-water periods.

Our analysis indicated a contrast between mechanisms influencing δ^{13}C-DIC in streams and in floodplain rivers (Fig. 8). Physical and biological processes control δ^{13}C-DIC throughout the upstream-downstream gradient. However, whereas gas exchange with the atmosphere and groundwater inputs appear to be dominant controls of δ^{13}C-DIC in small streams, carbonate weathering and photosynthesis by cyanobacteria are particularly important in higher-order rivers. To fully evaluate physical and biological controls of δ^{13}C-DIC in streams and rivers,

Biogeosciences Discuss., doi:10.5194/bg-2015-558, 2016
Manuscript under review for journal Biogeosciences
Published: 18 January 2016

346 measurements of rates of algal primary production and respiration, gas exchange between the air
347 and water, and groundwater inputs would be needed. Our results also have implications for
348 future studies using $\delta^{13}C$ to investigate food web structure in rivers. Studies in temperate regions
349 with seasonal snow cover should take temporal shifts in $\delta^{13}C$-DIC into account. Failure to
350 consider temporal changes in $\delta^{13}C$-DIC can bias inferences about consumer-resource dynamics
351 (Woodland et al., 2012). Finally, food web models that incorporate patterns of spatial variation in
352 $\delta^{13}C$-DIC (Rasmussen et al., 2009; Rasmussen, 2010) are dependent upon an underlying isotope
353 gradient. Thus, the applicability of these models in many aquatic ecosystems has been
354 questioned (Layman et al., 2012). Our GAMM analysis showed a positive relationship between
355 Strahler order and $\delta^{13}C$-DIC, indicating that headwaters have low $\delta^{13}C$-DIC values relative to
356 downstream reaches in most river systems. The rivers with the most pronounced upstream-
357 downstream gradients in $\delta^{13}C$-DIC will be those in which headwaters have high levels of pCO_2
358 (Fig. 8). Incorporation of spatial variation in $\delta^{13}C$-DIC in future lotic food web studies will thus
359 provide insights about the ecology of aquatic organisms, including movements and assimilation
360 of organic matter from alternative production sources.
361
362
363
364
365
366
367
368

Biogeosciences Discuss., doi:10.5194/bg-2015-558, 2016
Manuscript under review for journal Biogeosciences
Published: 18 January 2016

369 **Appendix A: Sources of data for the literature review**

Watershed	Location	Citation
Amazon	South America	Mayorga et al., 2005
Brazos	Texas, USA	Zeng et al., 2011
Chico	Argentina	Brunet et al., 2005
Chubut	Argentina	Brunet et al., 2005
Colorado	Argentina	Brunet et al., 2005
Congo	Africa	Bouillon et al., 2012; Bouillon et al., 2014
Coyle	Argentina	Brunet et al., 2005
Danube	Europe	Kanduč et al., 2007
Deseado	Argentina	Brunet et al., 2005
Ems	Germany	Stögbauer et al., 2008
Fraser	British Columbia, Canada	Cameron et al., 1995; Spence and Telmer, 2005
Gallegos	Argentina	Brunet et al., 2005
Ganges-Brahmaputra	Asia	Galy and France-Lanord, 1999
Han	Korea	Lee et al., 2007
Indus	Asia	Karim and Veizer, 2000
Khwai	Africa	Akoko et al., 2013
Lagan	Ireland	Barth et al., 1998
Mackenzie	Canada	Hitchon and Krouse, 1972; Reeder et al., 1972
Murray	Australia	Cartwright, 2010
Nass	British Columbia, Canada	Spence and Telmer, 2005
Negro	Argentina	Brunet et al., 2005
Okavango	Africa	Akoko et al., 2013
Pearl	Asia	Zhang et al., 2009
Rhine	Europe	Flintrop et al., 1996; Stögbauer et al., 2008
Rhône	Europe	Aucour et al., 1999
Santa Cruz	Argentina	Brunet et al., 2005
Skeena	British Columbia, Canada	Spence and Telmer, 2005
Squamish	British Columbia, Canada	Spence and Telmer, 2005
St. Lawrence	Canada and USA	Yang et al., 1996; Telmer and Veizer, 1999; Hélie et al., 2002
Tana	Kenya	Bouillon et al., 2009; Tamooh et al., 2013
Vistula	Poland	Wachniew, 2006

370

371

372

Biogeosciences Discuss., doi:10.5194/bg-2015-558, 2016
Manuscript under review for journal Biogeosciences
Published: 18 January 2016

Acknowledgments

We are grateful to E. Mayorga for providing data from the Amazon River Basin and to P. Massicotte for assistance in determining Strahler order. Financial support came from the Plan d'Action Saint-Laurent (PASL) to YP, Natural Sciences and Engineering Research Council of Canada (NSERC) Discovery Grants to MAR and GC, and an NSERC Banting Postdoctoral Fellowship to KAR.

References

Abril. G., Bouillon, S., Darchambeau, F., Teodoru, C.R., Marwick, T.R., Tamooh, F., Ochieng Omengo, F., Geeraert, N., Deirmendjian, L., Polsenaere, P., and Borges, A.V. Technical note: Large overestimation of pCO_2 calculated from pH and alkalinity in acidic, organic-rich freshwaters, Biogeosciences, 12, 67–78, 2015.

Akoko, E., Atekwana, E.A., Cruse, A.M., Molwalefhe, L., and Masamba, W.R.L. River-wetland interaction and carbon cycling in a semi-arid riverine system: the Okavango Delta, Botswana, Biogeochemistry, 114, 359–380, 2013.

Aravena, R., Schiff, S.L., Trumbore, S.E., Dillon, P.J., and Elgood, R. Evaluating dissolved inorganic carbon cycling in a forested lake watershed using carbon isotopes, Radiocarbon, 34, 636–645, 1992.

Aucour, A.M., Sheppard, S.M.F., Guyomar, O., and Wattelet, J, Use of ^{13}C to trace origin and cycling of inorganic carbon in the Rhône river system, Chem. Geol., 159, 87–105, 1999.

Aufdenkampe, A.K., Mayorga, E., Raymond, P.A., Melack, J.M., Doney, S.C., Alin, S.R., Aalto, R.E., and Yoo, K. Riverine coupling of biogeochemical cycles between land, oceans, and atmosphere, Front. Ecol. Environ., 9, 53–60, 2011.

396 Bade, D.L., Carpenter, S.R., Cole, J.J., Hanson, P.C., and Hesslein, R.H. Controls of δ^{13}C-DIC in
397 lakes: Geochemistry, lake metabolism, and morphometry, Limnol. Oceanogr., 49, 1160–1172,
398 2004.
399 Barnett, A.G., and Dobson, A.J. Analysing seasonal health data. Springer, Berlin Heidelberg,
400 Springer, 2010.
401 Barth, J.A.C., Veizer, J., and Mayer, B. Origin of particulate organic carbon in the upper St.
402 Lawrence: isotopic constraints, Earth Planet Sci. Lett., 162, 111–121, 1998.
403 Battin, T.J., Kaplan, L.A., Findlay, S., Hopkinson, C.S., Marti, E., Packman, A.I., Newbold, J.D.,
404 and Sabater, F. Biophysical controls on organic carbon fluxes in fluvial networks, Nature
405 Geosci., 1, 95–100, 2008.
406 Bertrand, M., Cabana, G., Marcogliese, D.J., and Magnan, P. Estimating the feeding range of a
407 mobile consumer in a river-flood plain system using δ^{13}C gradients and parasites, J. Anim. Ecol.,
408 80, 1313–1323, 2011.
409 Bouillon, S., Abril, G., Borges, A.V., Dehairs, F., Govers, G., Hughes, H.J., Merckx, R.,
410 Meysman, F.J.R., Nyunja, J., Osburn, C., and Middelburg, J.J. Distribution, origin and cycling of
411 carbon in the Tana River (Kenya): a dry season basin-scale survey from headwaters to the delta,
412 Biogeosciences, 6, 2475–2993, 2009.
413 Bouillon, S., Yambélé, A., Gillikin, D.P., Teodoru, C., Darchambeau, F., Lambert, T., and
414 Borges, A.V. Contrasting biogeochemical characteristics of the Oubangui River and tributaries
415 (Congo River basin), Sci. Rep., 4, 5402, doi:10.1038/srep05402, 2014.
416 Bouillon, S., Yambélé, A., Spencer, R.G.M., Gillikin, D.P., Hernes, P.J., Six, J., Merckx, R., and
417 Borges, A.V. Organic matter sources, fluxes and greenhouse gas exchange in the Oubangui
418 River (Congo River basin), Biogeosciences, 9, 2045–2062, 2012.

419 Boutton, T.W. Stable carbon isotope ratios of natural materials: II. Atmospheric, terrestrial,
420 marine, and freshwater environments, in: Carbon isotope techniques, edited by: Coleman, D.C.,
421 and Fry, B., San Diego, Academic Press, 173–185, 1991.
422 Brunet, F., Gaiero, D., Probst, J.L., Depetris, P.J., Lafaye, F.G., and Stille, P. $\delta^{13}C$ tracing of
423 dissolved inorganic carbon sources in Patagonian rivers (Argentina), Hydrol. Process., 19, 3321–
424 3344, 2005.
425 Butman, D., and Raymond, P.A. Significant efflux of carbon dioxide from streams and rivers in
426 the United States, Nature Geosci., 4, 839–842, 2011.
427 Cameron, E.M., Hall, G.E.M., Veizer, J., and Krouse, H.R. Isotopic and elemental
428 hydrogeochemistry of a major river system: Fraser River, British Columbia, Canada, Chem.
429 Geol., 122, 149–169, 1995.
430 Cartwright, I. The origins and behaviour of carbon in a major semi-arid river, the Murray River,
431 Australia, as constrained by carbon isotopes and hydrochemistry, Appl. Geochem., 25, 1734–
432 1745, 2010.
433 Cole, J.J., Prairie, Y.T., Caraco, N.F., McDowell, W.H., Tranvik, L.J., Striegl, R.G., Duarte,
434 C.M., Kortelainen, P., Downing, J.A., Middelburg, J.J., and Melack, J. Plumbing the global
435 carbon cycle: integrating inland waters into the terrestrial carbon budget, Ecosystems, 10, 171–
436 184, 2007.
437 Dawson, J.J.C., Bakewell, C., and Billett, M.F. Is in-stream processing an important control on
438 spatial changes in carbon fluxes in headwater catchments? Sci. Total. Environ., 265, 153–167,
439 2001.
440 Dawson, J.J.C., Billett, M.F., Hope, D., Palmer, S.M., and Deacon, C.M. Sources and sinks of
441 aquatic carbon in a peatland stream continuum, Biogeochemistry, 70, 71–92, 2004.

Biogeosciences Discuss., doi:10.5194/bg-2015-558, 2016
Manuscript under review for journal Biogeosciences
Published: 18 January 2016

442 Devol, A.H., Quay, P.D., Richey, J.E., and Martinelli, L.A. The role of gas exchange in the
443 inorganic carbon, oxygen, and ^{222}Rn budgets of the Amazon River, Limnol. Oceanogr., 32, 235–
444 248, 1987.
445 Finlay, J.C. Controls of streamwater dissolved inorganic carbon dynamics in a forested
446 watershed, Biogeochemistry, 62, 231–252, 2003.
447 Flintrop, C., Hohlmann, B., Jasper, T., Korte, C., Podlaha, O.G., Scheele, S., and Veizer, J.
448 Anatomy of pollution: rivers of north Rhine-Westphalia, Germany, Am. J. Sci., 296, 58–98,
449 1996.
450 Galy, A., and France-Lanord, C. Weathering processes in the Ganges-Brahmaputra basin and the
451 riverine alkalinity budget, Chem. Geol., 159, 31–60, 1999.
452 Gray, D.P., Harding, J.S., Elberling, B., Horton, T., Clough, T.J., and Winterbourn, M.J. Carbon
453 cycling in floodplain ecosystems: out-gassing and photosynthesis transmit soil delta C-13
454 gradient through stream food webs, Ecosystems, 14, 583–597, 2011.
455 Hélie, J.F., Marcel, C.H., and Rondeau, B. Seasonal changes in the sources and fluxes of
456 dissolved inorganic carbon through the St. Lawrence River - isotopic and chemical constraint,
457 Chem. Geol., 186, 117–138, 2002.
458 Herczog, A.L., and Fairbanks, R.G. Anomalous carbon isotope fractionation between
459 atmospheric CO_2 and dissolved inorganic carbon induced by intense photosynthesis, Geochim.
460 Cosmochim. Acta, 51, 895–899, 1987.
461 Hitchon, B., and Krouse, H.R. Hydrogeochemistry of the surface waters of the Mackenzie River
462 drainage basin, Canada - III. Stable isotopes of oxygen, carbon, and sulphur, Geochim.
463 Cosmochim. Acta, 36, 1337–1357, 1972.

Biogeosciences Discuss., doi:10.5194/bg-2015-558, 2016
Manuscript under review for journal Biogeosciences
Published: 18 January 2016

464 Johnson, M.S., Lehmann, J., Riha, S.J., Krusche, A.V., Richey, J.E., Ometto, J.P.H.B., and
465 Couto, E.G. CO_2 efflux from Amazonian headwater streams represents a significant fate for deep
466 soil respiration, Geophys. Res. Lett., 35, L17401, doi:10.1029/2008GG034619, 2008.
467 Johnson, M.S., Lehmann, J., Selva, E.C., Abdo, M., Riha, S., and Couto, E.G. (2006) Organic
468 carbon fluxes within and streamwater exports from headwater catchments in the southern
469 Amazon, Hydrol. Process., 20, 2599–2614
470 Jones, J.B. Jr., and Mulholland, P.J. Influence of drainage basin topography and elevation on
471 carbon dioxide and methane supersaturation of stream water, Biogeochemistry, 40, 57–72, 1998.
472 Jones, J.B. Jr., Stanley, E.H., and Mulholland, P.J. Long-term decline in carbon dioxide
473 supersaturation in rivers across the contiguous United States, Geophys. Res. Lett., 30, 1495–
474 1499, 2003.
475 Kanduč, T., Szramek, K., Ogrinc, N., and Walter, L.M. Origin and cycling of riverine inorganic
476 carbon in the Sava River watershed (Slovenia) inferred from major solutes and stable carbon
477 isotopes, Biogeochemistry, 86, 137–154, 2007.
478 Karim, A., and Veizer, J. Weathering processes in the Indus River Basin: implications from
479 riverine carbon, sulfur, oxygen, and strontium isotopes, Chem. Geol., 170, 153–177, 2000.
480 Karlsson, J., Ask, J., and Jansson, M. Winter respiration of allochthonous and autochthonous
481 organic carbon in a subarctic clear-water lake, Limnol. Oceanogr., 53, 947–954, 2008.
482 Kendall, C., and Doctor, D.H. Stable isotope applications in hydrologic studies, Treatise on
483 Geochemistry, 5, 319–364, 2003.
484 Layman, C.A., Araujo, M.S., Boucek, R., Hammerschlag-Peyer, C.M., Harrison, E., Jud, Z.R.,
485 Matich, P., Rosenblatt, A.E., Vaudo, J.J., Yeager, L.A., Post, D.M., and Bearhop, S. Applying

stable isotopes to examine food web structure: an overview of analytical tools, Biological Reviews, 87, 542–562, 2012.

Lee, K.S., Ryu, J.S., Ahn, K.H., Chang, H.W., and Lee, D. Factors controlling carbon isotope ratios of dissolved inorganic carbon in two major tributaries of the Han River, Korea. Hydrol. Process., 21, 500–509, 2007.

Lehner, B., Verdin, K., and Jarvis, A. New global hydrography derived from spaceborne elevation data, Eos, Trans. Amer. Geophys. Union, 89, 93–94, 2008.

Levin, I., Kromer, B., Wagenback, D., and Munnich, K.O. Carbon isotope measurements of atmospheric CO_2 at a coastal station in Antarctica, Tellus, 39B, 89–95, 1987.

Livingstone, D.A. Chemical composition of rivers and lakes, U.S. Geol. Survey Prof. Pap., 40-G, 1–64, 1963.

Mayorga, E., Aufdenkampe, A.K., Masiello, C.A., Krusche, A.V., Hedges, J.I., Quay, P.D., Richey, J.E., and Brown, T.A. Young organic matter as a source of carbon dioxide outgassing from Amazonian rivers, Nature, 436, 538–541, 2005.

McKenzie, J.A. Carbon isotopes and productivity in the lacustrine and marine environment, in: Chemical Processes in Lakes, edited by: Stumm, W., New York, John Wiley & Sons, 99–118, 1985.

Meyer, J.L. A blackwater perspective on riverine ecosystems. BioScience, 40, 643–651, 1990.

Mulholland, P.J., Fellows, C.S., Tank, J.L., Grimm, N.B., Webster, J.R., Hamilton, S.K., Marti, E., Ashkenas, L., Bowden, W.B., Dodds, W.K., McDowell, W.H., Paul, M.J., and Peterson, B.J. Inter-biome comparison of factors controlling stream metabolism. Freshw. Biol., 46, 1503–1517, 2001.

508 Paerl, H.W., and Ustach, J.F. Blue-green algal scums: an explanation for their occurrence during
509 freshwater blooms, Limnol. Oceanogr., 27, 212–217, 1982.
510 R Core Team. R: A language and environment for statistical computing. Vienna, Austria, R
511 Foundation for Statistical Computing, 2015.
512 Rasmussen, J.B. Estimating terrestrial contribution to stream invertebrates and periphyton using
513 a gradient-based mixing model for $\delta^{13}C$, J. Anim. Ecol., 79, 393–402, 2010.
514 Rasmussen, J.B., Trudeau, V., and Morinville, G. Estimating the scale of fish feeding
515 movements in rivers using $\delta^{13}C$ signature gradients. J. Anim. Ecol., 78, 674–685, 2009.
516 Raymond, P.A., Caraco, N.F., and Cole, J.J. Carbon dioxide concentration and atmospheric flux
517 in the Hudson River, Estuaries, 20, 381–390, 1997.
518 Rebsdorf, A., Thyssen, N., and Erlandsen, M. Regional and temporal variation in pH, alkalinity,
519 and carbon dioxide in Danish streams, related to soil type and land use, Freshw. Biol., 25, 419–
520 435, 1991.
521 Reeder, S.W., Hitchon, B., and Levinson, A.A. Hydrogeochemistry of the surface waters of the
522 Mackenzie River drainage basin, Canada - I. Factors controlling inorganic composition,
523 Geochim. Cosmochim. Ac., 36, 825–865, 1972.
524 Richey, J.E., Melack, J.M., Aufdenkampe, A.K., Ballester, V.M., and Hess, L.L. Outgassing
525 from Amazonian rivers and wetlands as a large tropical source of atmospheric CO_2, Nature, 416,
526 617–620, 2002.
527 Roussel, J.M., Perrier, C., Erkinaro, J., Niemelä, E., Cunjak, R.A., Huteau, D., and Riera, P.
528 Stable isotope analyses on archived fish scales reveal the long-term effect of nitrogen loads on
529 carbon cycling in rivers, Glob. Change Biol., 20, 523–530, 2013.

530 Spence J., and Telmer, K. The role of sulfur in chemical weathering and atmospheric CO_2 fluxes:
531 evidence from major ions, $\delta^{13}C_{DIC}$, and $\delta^{34}S_{SO4}$ in rivers of the Canadian Cordillera. Geochim.
532 Cosmochim. Ac., 69, 5441–5458, 2005.
533 Stögbauer, A., Strauss, H., Arndt, J., Marek, V., Einsiedl, F., and van Geldern, R. Rivers of
534 North-Rhine Westphalia revisited: tracing changes in river chemistry, Appl. Geochem., 23,
535 3290–2304, 2008.
536 Striegl, R.G., Kortelainen, P., Chanton, J.P., Wickland, K.P., Bugna, G.C., and Rantakari, M.
537 Carbon dioxide partial pressure and ^{13}C content of north temperate and boreal lakes at spring ice
538 melt, Limnol. Oceanogr., 46, 941–945, 2001.
539 Stumm, W., and Morgan, J.J. Aquatic chemistry: chemical equilibria and rates in natural waters.
540 New York, John Wiley & Sons, 2012.
541 Tamooh, F., Borges, A.V., Meysman, F.J.R., Meersche, Van Den Meersche, K., Dehairs, F.,
542 Merckx, R., and Bouillon, S. Dynamics of dissolved inorganic carbon and aquatic metabolism in
543 the Tana River basin, Kenya. Biogeosciences, 10, 6911–2928, 2013.
544 Telmer, K.H., and Veizer, J. Carbon fluxes, pCO_2 and substrate weathering in a large northern
545 river basin, Canada: carbon isotope perspectives, Chem. Geol., 159, 61–86, 1999.
546 Teodoru, C.R., del Giorgio, P.A., Prairie, Y.T., and Camire, M. Patterns in pCO_2 in boreal
547 streams and rivers of northern Quebec, Canada, Global Biogeochem. Cy., 23, GB2012,
548 doi:10.1029/2008GB003404, 2009.
549 Wachniew, P. Isotopic composition of dissolved inorganic carbon in a large polluted river: the
550 Vistula, Poland, Chem. Geol., 233, 293–308, 2006.
551 Wanninkhof, R., Mulholland, P.J., and Elwood, J.W. Gas exchange rates for a first-order stream
552 determined with natural tracers, Water Resour. Res., 26, 1621–1630, 1990.

Biogeosciences Discuss., doi:10.5194/bg-2015-558, 2016
Manuscript under review for journal Biogeosciences
Published: 18 January 2016

553 Wood, S.N. Generalized additive models: an introduction with R. Boca Raton, Chapman and
554 Hall/CRC, 2006.
555 Wood, S.N. Fast stable restricted maximum likelihood and marginal likelihood estimation of
556 semiparametric generalized linear models, J. R. Stat. Soc. Series B 73, 3-36, 2011.
557 Woodland, R.J., Rodríguez, M.A., Magnan, P., Glémet, H., and Cabana, G. Incorporating
558 temporally dynamic baselines in isotopic mixing models, Ecology, 93, 131–144, 2012.
559 Wynn, J.G., and Bird, M.I. C4-derived soil organic carbon decomposes faster than its C3
560 counterpart in mixed C3/C4 soils, Glob. Change Biol., 13, 1–12, 2007.
561 Yang, C., Telmer, K., and Veizer, J. Chemical dynamics of the "St. Lawrence" riverine system:
562 δD_{H2O}, $\delta^{18}O_{H2O}$, $\delta^{13}C_{DIC}$, $\delta^{34}S_{sulfate}$, and dissolved $^{87}Sr/^{86}Sr$, Geochim. Cosmochim. Ac., 60, 851–
563 866, 1996.
564 Zeng, F.W., Masiello, C.A., and Hockaday, W.C. Controls on the origin and cycling of riverine
565 dissolved inorganic carbon in the Brazos River, Texas, Biogeochemistry, 104, 275–291, 2011.
566 Zhang, J., Quay, P.D., and Wilbur, D.O. Carbon isotope fractionation during gas-water exchange
567 and dissolution of CO_2. Geochim. Cosmochim. Ac., 59, 107–114, 1995.

Biogeosciences Discuss., doi:10.5194/bg-2015-558, 2016
Manuscript under review for journal Biogeosciences
Published: 18 January 2016

568 Table 1. Quantitative output of the generalized additive mixed models (GAMM) of $\Delta\delta^{13}$C-DIC,
569 including information on units and model effects. Estimated degrees of freedom = edf. The
570 GAMM explained a total of 85.2% of the deviance.

Model term	Unit	Effect	Estimate	Std. Error	edf	Standard deviation	p-value
Intercept			-10.07	0.63			<0.001
Strahler order		Linear	0.27	0.09			<0.01
Dissolved inorganic carbon (DIC)	mmol/L	Smooth			6.4		<0.001
Elevation	masl	Smooth			5.0		<0.001
Day-of-year × Latitude		Smooth			19.9		<0.001
Day-of-year × Latitude		Smooth			14.1		<0.001
Distance from river mouth	km	Smooth			7.1		<0.001
Watershed		Random			11.7	1.7	<0.001
River		Random			97.1	1.5	<0.001

571
572
573
574
575
576
577
578
579
580

Biogeosciences Discuss., doi:10.5194/bg-2015-558, 2016
Manuscript under review for journal Biogeosciences
Published: 18 January 2016

581 Table 2. Quantitative output of the generalized additive mixed models (GAMM) of δ^{13}C-DIC,
582 including information on units and model effects. Estimated degrees of freedom = edf. The
583 GAMM explained a total of 90.6% of the deviance.

Model term	Unit	Effect	Estimate	Std. Error	edf	Standard deviation	p-value
Intercept			-10.76	0.58			<0.001
Strahler order		Linear	0.27	0.09			<0.01
pH		Smooth			5.9		<0.001
Dissolved inorganic carbon (DIC)	mmol/L	Smooth			7.1		<0.001
Partial pressure of dissolved CO_2 (pCO_2)	ppmv	Smooth			3.8		<0.001
Elevation	masl	Smooth			5.1		<0.001
Day-of-year × Latitude		Smooth			21.0		<0.001
Day-of-year × Latitude		Smooth			15.2		<0.001
Distance from river mouth	km	Smooth			6.4		<0.001
Watershed		Random			9.9	1.4	<0.001
River		Random			104.5	1.6	<0.001

584
585
586
587
588
589
590
591
592
593

Biogeosciences Discuss., doi:10.5194/bg-2015-558, 2016
Manuscript under review for journal Biogeosciences
Published: 18 January 2016

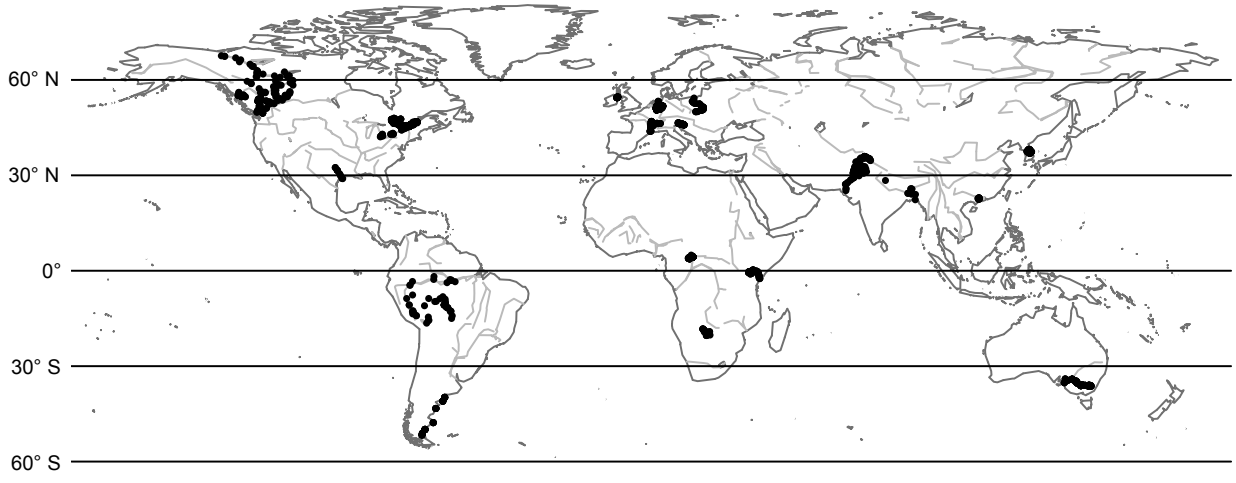

594

595 Figure 1. Map of the study sites included in the literature survey. Major world rivers are shown

596 in light grey.

Biogeosciences Discuss., doi:10.5194/bg-2015-558, 2016
Manuscript under review for journal Biogeosciences
Published: 18 January 2016

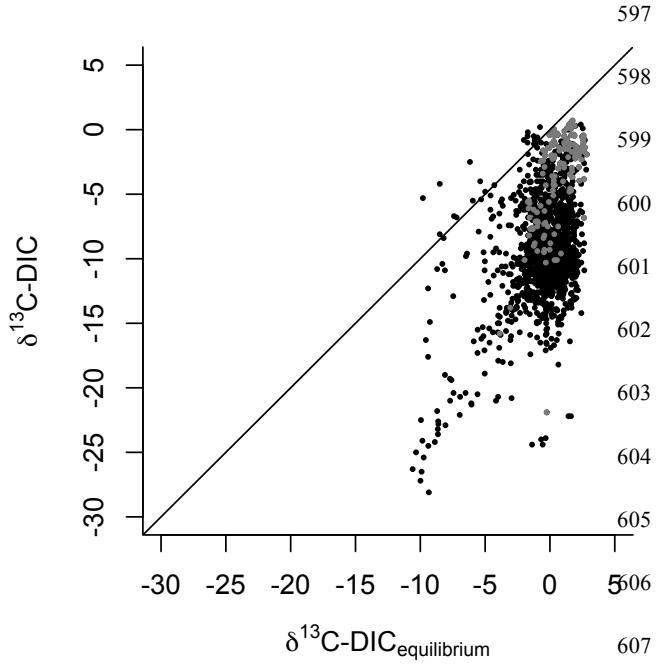

608 Figure 2. The relationship between δ^{13}C-DIC$_{equilibrium}$ (the δ^{13}C signature of DIC at isotopic
609 equilibrium with the atmosphere) and δ^{13}C-DIC in rivers. Grey symbols are from rivers with
610 Strahler order = 8 and black symbols are from rivers with Strahler order < 8. The line indicates
611 the 1:1 relationship.

612

613

614

615

616

617

618

619

Biogeosciences Discuss., doi:10.5194/bg-2015-558, 2016
Manuscript under review for journal Biogeosciences
Published: 18 January 2016

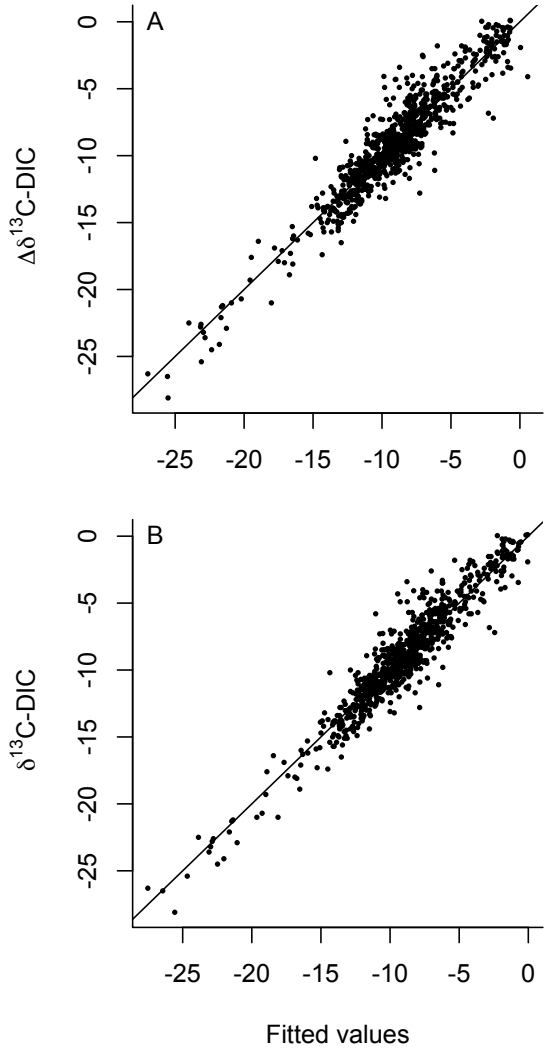

638

639 Figure 3. Plots of fitted versus observed values for $\Delta\delta^{13}$C-DIC (A) and δ^{13}C-DIC (B).

640

Biogeosciences Discuss., doi:10.5194/bg-2015-558, 2016
Manuscript under review for journal Biogeosciences
Published: 18 January 2016

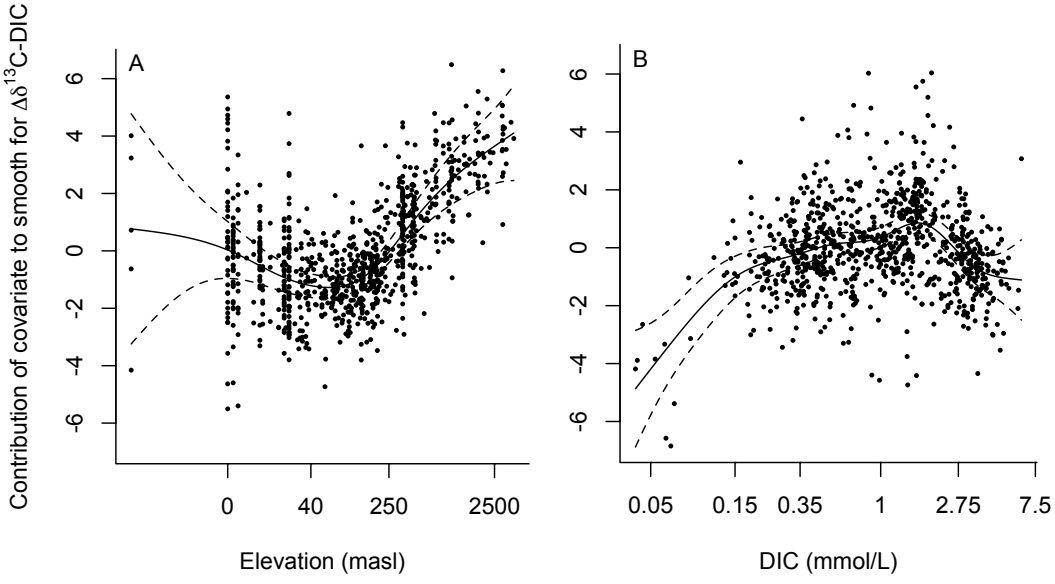

641

642

643 Figure 4. Smooth function (curve) derived from the generalized additive mixed model (GAMM)
644 fit for relationships between $\Delta\delta^{13}$C-DIC and elevation (meters above sea level, A) and dissolved
645 inorganic carbon (DIC) concentrations (mmol/L, B). Dashed curves represent 95% confidence
646 intervals for the smooth. Partial residuals (points) are also shown. Higher $\Delta\delta^{13}$C-DIC values
647 indicate that δ^{13}C-DIC is closer to isotopic equilibrium with the atmosphere. Note that the
648 smooth function y-axis is centered to zero mean.

649

650

651

652

653

654

Biogeosciences Discuss., doi:10.5194/bg-2015-558, 2016
Manuscript under review for journal Biogeosciences
Published: 18 January 2016

655

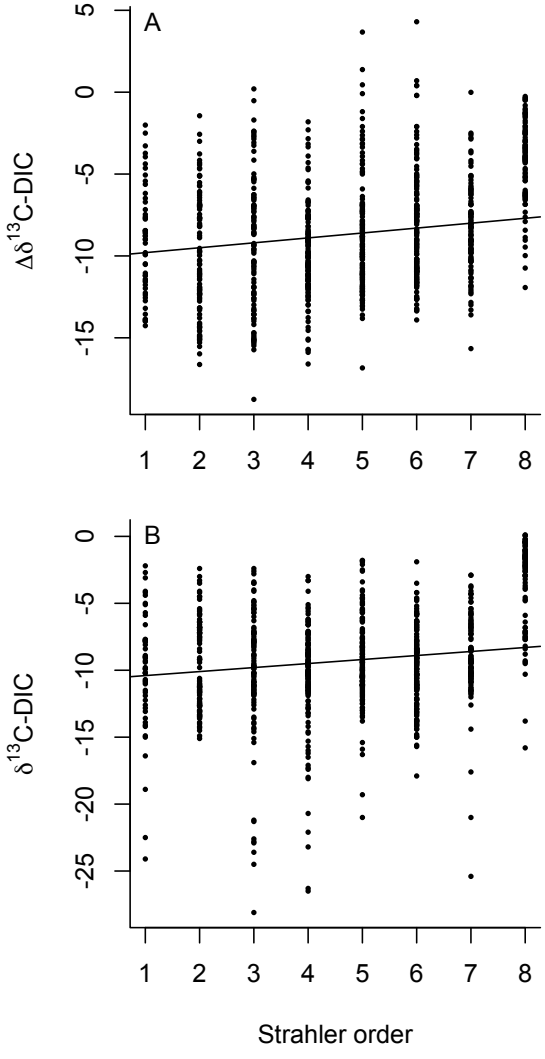

674 Figure 5. Relationships between Strahler order and $\Delta\delta^{13}$C-DIC (A) and δ^{13}C-DIC (B). The
675 regression lines determined by the coefficients of the generalized additive mixed models
676 (GAMMs) are shown.

677

Biogeosciences Discuss., doi:10.5194/bg-2015-558, 2016
Manuscript under review for journal Biogeosciences
Published: 18 January 2016

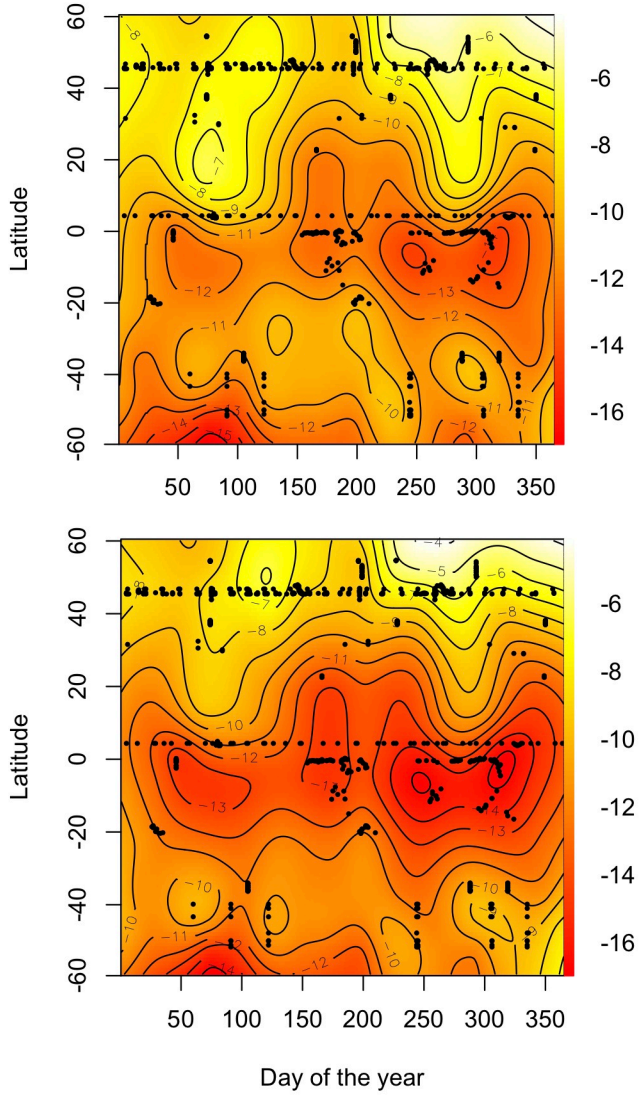

696

697 Figure 6. Contour plots showing the seasonal variation in fitted $\Delta\delta^{13}$C-DIC (top) and δ^{13}C-DIC
698 (bottom) at different latitudes. Lighter colors indicate higher $\Delta\delta^{13}$C-DIC values (values closer to
699 atmospheric equilibrium) for the top plot and higher δ^{13}C-DIC values for the bottom plot.

700

Biogeosciences Discuss., doi:10.5194/bg-2015-558, 2016
Manuscript under review for journal Biogeosciences
Published: 18 January 2016

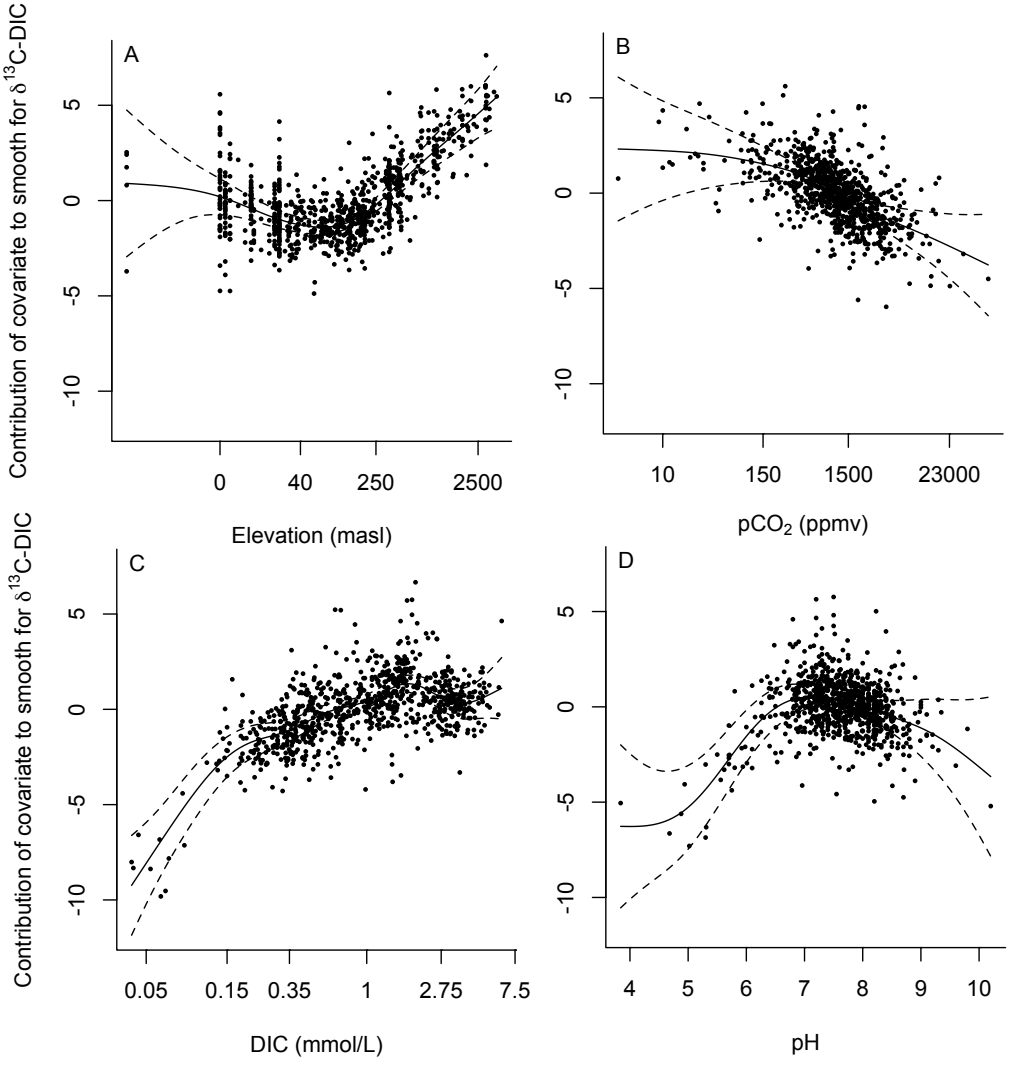

Figure 7. Smooth function (curve) derived from the generalized additive mixed model (GAMM) fit for relationships between rescaled δ^{13}C-DIC and elevation (masl, A), pCO_2 (ppmv, B), dissolved inorganic carbon (DIC) concentrations (mmol/L, C), and pH (D). Dashed curves represent 95% confidence intervals for the smooth. Partial residuals (points) are also shown. Note that the smooth function y-axis is centered to zero mean.

Biogeosciences Discuss., doi:10.5194/bg-2015-558, 2016
Manuscript under review for journal Biogeosciences
Published: 18 January 2016

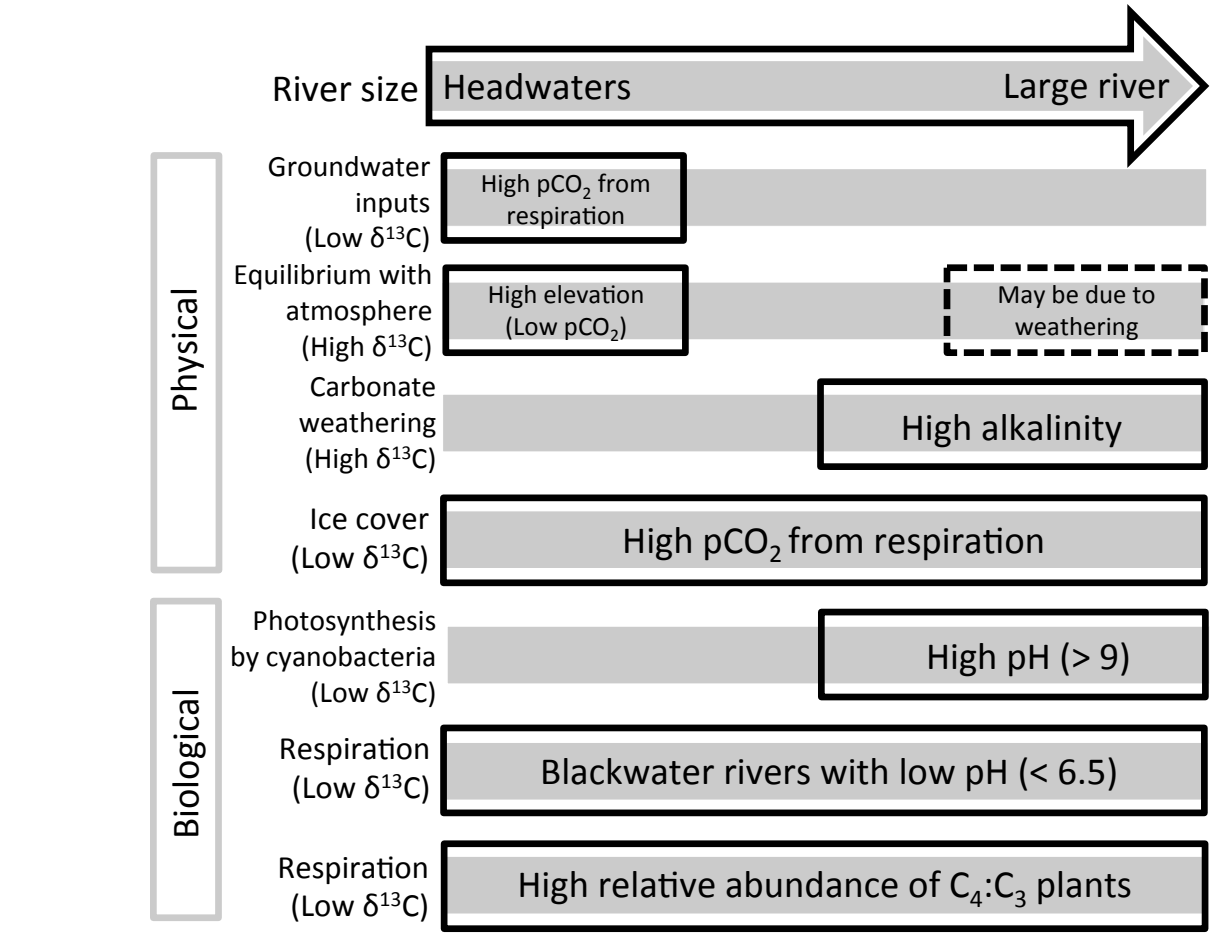

708

709

710 Figure 8. Schematic diagram showing dominant physical and biological controls of δ^{13}C-DIC in
711 rivers throughout the world. The grey figures represent the longitudinal river gradient. The black
712 outlines indicate the relative importance of various processes influencing δ^{13}C-DIC along the
713 upstream-downstream gradient. Patterns in pCO_2 along the river gradient also are shown. The
714 dotted outline indicates that floodplain rivers are near isotopic equilibrium with the atmosphere,
715 but this may be because carbonate weathering also is associated with high δ^{13}C-DIC values.